Ecological Indicators 61 (2016) 317–327

Contents lists available at ScienceDirect

Ecological Indicators

journal homepage: www.elsevier.com/locate/ecolind

A new view on EU agricultural landscapes: Quantifying patchiness to assess farmland heterogeneity

Christof J. Weissteiner[1], Celia García-Feced[2], Maria Luisa Paracchini*

European Commission, Joint Research Centre (JRC), Institute for Environment and Sustainability, Via Enrico Fermi, 2749, 21027 Ispra, VA, Italy

ARTICLE INFO

Article history:
Received 17 February 2015
Received in revised form
17 September 2015
Accepted 22 September 2015
Available online 7 November 2015

Keywords:
Farmland heterogeneity
Patch size
Field size
Texture
Landscape metrics

ABSTRACT

Mapping and assessment of ecosystem services in agricultural landscapes as required by the EU biodiversity policy need a better characterization of the given landscape typology according to its ecological and cultural values. Such need should be accommodated by a better discrimination of the landscape characteristics linked to the capacity of providing ecosystem services and socio-cultural benefits. Often, these key variables depend on the degree of farmland heterogeneity and landscape patterns. We employed segmentation and landscape metrics (edge density and image texture respectively), derived from a pan-European multi-temporal and multi-spectral remote sensing dataset, to generate a consistent European indicator of farmland heterogeneity, the Farmland Heterogeneity Indicator (FHI). We mapped five degrees of FHI on a wall-to-wall basis (250 m spatial resolution) over European agricultural landscapes including natural grasslands. Image texture led to a clear improvement of the indicator compared to the pure application of Edge Density, in particular to a better detection of small patches. In addition to deriving a qualitative indicator we attributed an approximate patch size to each class, allowing an indicative assessment of European field sizes. Based on CORINE land cover, we identified pastures and heterogeneous land cover classes as classes with the highest degree of FHI, while agroforestry and olive groves appeared less heterogeneous on average. We performed a verification based on a continental and regional scale, which resulted in general good agreement with independently derived data.

1. Introduction

Agro-ecosystems are the result of human activities aimed at producing food, feed, fibres and energy. This primary output of agriculture is classified in the ecosystem services frame (MA, 2005) as provisioning ecosystem service. Alongside with agricultural biomass production, farming practices also impact on the capacity of agro-ecosystems to supply regulating and cultural ecosystem services, some of which directly support agricultural production (i.e. soil fertility, water availability, pollination, pest control, soil erosion mitigation) (Bommarco et al., 2013). Farmland biodiversity is hosted to a varying degree in all agricultural landscapes, being the result of thousands of years of agricultural practices. It is generally enhanced and maintained by extensive practices and threatened by intensification (Benton et al., 2003). In particular fragmentation and conversion of natural habitats, removal of landscape elements (e.g. hedges, tree lines, ridges) increase of field size and reduction of crop diversity have contributed to species decline (Donald et al., 2006), including species that are functional to agricultural production (Haenke et al., 2014; Le Féon et al., 2010). From the European policy side, the supply of ecosystem services and biodiversity conservation within farmland is fostered by the EU Biodiversity Strategy to 2020 (European Commission, 2011) and the Common Agricultural Policy (CAP) with its so-called Greening measures (European Union, 2013).

Several studies have tried to assess and/or map the degree to which selected agricultural land characteristics support biodiversity and ecosystem service provision (Billeter et al., 2008; Donald et al., 2006; Herzog et al., 2006; Overmars et al., 2014; Roschewitz et al., 2005). The ecological role of habitat diversity and field edges as source and sink of farmland biodiversity (including functional biodiversity) has been demonstrated by several authors (Gabriel et al., 2006; Jentsch et al., 2012; Kaule and Krebs, 1989; Marshall and Moonen, 2002; Wagner et al., 2000). Recognized important features playing an important role in this respect are linear landscape elements, such as ditches, hedge and tree lines, and grass margins (García-Feced et al., 2015; Van der Zanden et al., 2013). An enhanced supply of regulating ecosystem services and biodiversity

* Corresponding author. Tel.: +39 0332 789897.
E-mail addresses: christof.weissteiner@ext.jrc.ec.europa.eu (C.J. Weissteiner), celia.garcia.feced@upm.es (C. García-Feced), luisa.paracchini@jrc.ec.europa.eu (M.L. Paracchini).
[1] Tel.: +39 0332 786787.
[2] Tel.: +39 0332 789897.

http://dx.doi.org/10.1016/j.ecolind.2015.09.032
1470-160X/

maintenance is linked to the spatial arrangement of (such) features that increase habitat availability, individual movement and species dispersal when distributed across the landscape with sufficient density and connectivity (Landis et al., 2000; Wiens et al., 1993). The importance of the landscape scale in the regulation of biodiversity processes has been underlined by several authors (Ernoult et al., 2003; Hamer et al., 2006; Tscharntke et al., 2005); however, a lack of information on the spatial configuration of the agricultural landscape on the EU scale limits the possibility of assessing its ecological value at the continental level. An existing assessment (Paracchini et al., 2008) in fact relies on CORINE land cover data (EEA, 2007) which, due to its inherent degree of generalization, does not fully capture the complexity of agricultural landscapes. Recent studies (García-Feced et al., 2015; Van der Zanden et al., 2013) provide information on the presence of landscape features but information on other structural parameters such as field size or patch distribution is still missing. An indicator is therefore needed to fill this gap and to increase the detail of spatial characterization provided by land use maps. This proxy needs to (i) be robust (e.g. insensitive to comparable sensors) and repeatable to be monitored in time, (ii) be detailed enough to account for local particularities and (iii) cover areas of continental extent at the same time. Moreover, the approach of proxy derivation should be (iv) consistent across the whole area, and (v) economically feasible (preferably with no or minimal cost, e.g. based on free available source data). Multispectral remote sensing images fulfil most of these requirements, being suited in particular for the detection of changes in reflectance between spectrally homogeneous features and are thus particularly effective in the detection of field edges and habitat boundaries.

Given the ecological importance of structural elements, field size and patch distribution, and further considering the requirements of the indicator, a remote sensing-based indicator-based on edge density seems adequate. Such edges are both positively correlated with the edge density of classically defined patches (see Section 2.2 for definition) that can be detected in a multispectral image. Therefore, in this study we propose a new patch indicator, supposed to deliver a qualitative (related to degree of patchiness) and up to a certain degree a semi-quantitative assessment indicator (related to approximate field size) of the structure of European agricultural areas. The proposed indicator is based on an edge density metric combined with a parallel-derived texture-based measure. Both metrics are combined to a single indicator called FHI or Farmland Heterogeneity Indicator. FHI can be considered an improved Edge Density of patch borders, based on a combination of spectral *and* textural data as promoted by Chica-Olmo and Abarca-Hernández (2000), while improving the spatial extent of similar works (Kuemmerle et al., 2009; Rydberg and Borgefors, 2001) which cover smaller regions.

2. Materials and methods

2.1. Data

As base data for this study we used Image 2006 (Soille, 2008), a pan-European mosaic, providing top-of-atmosphere (TOA) reflectance of four pre-processed spectral bands in the green, red, near-infrared and mid-infrared spectrum, derived from the satellite sensors IRS P6 LISS-III, SPOT 4 and SPOT 5, and centred in the year 2006. A total of 2004 images were mosaicked for the first coverage of the mosaic (COV1), temporally centred in the early period of the vegetation period (spring, early summer), and 1,561 images for the second coverage (COV2) of the mosaic, temporally centred in the later period of the vegetation period (late summer, autumn). Details about data, pre-processing, cloud detection, accuracy, and the mosaicking method are reported by Soille (2008).

2.2. Methods

2.2.1. Farmland Heterogeneity Indicator (FHI) design

FHI aims to express a major part of the above-mentioned cultural and ecological values of landscape. FHI is intended for this purpose as a measure for the frequency of occurring patch variability within a defined area. To achieve this, we (i) performed a segmentation based on homogeneity criteria for spectral data, (ii) quantified patch edge density for a defined area A, (iii) calculated a textural indicator for A and (iv) combined both to create the FHI. A graphical overview of the FHI methodology is shown in Fig. 1. The core of the methodology is the segmentation and the parallel texture module, whose results are then fused: we considered the parallel approach beneficial since it consolidates the final results and enhances robustness. Moreover, following our empirical tests, texture still delivers meaningful results on areas with very small fields where the segmentation already fails. This led us to a complex fusion technique, which takes into account the asymmetry of data confidentiality.

In this work, a patch is defined as a homogeneous plot within the wider agricultural land, which assumes a different (remotely sensed) observable property from its surrounding neighbourhood, and, similar to Forman (1995), assumes an ecological meaning. The patch is detached from any cadastral meaning. According to this definition, patches do not necessarily represent agricultural fields, although most of them do so. A patch can also consist of remnant elements of semi-natural vegetation (forest, trees, hedges, edge of field and/or riparian buffer strips, etc.), small water bodies and wetlands, roads or even single buildings or rocks, which are not masked out by pre-stratification of agricultural areas. These elements, where encountered, are part of the definition of the FHI, intended as an indicator expressing heterogeneity, also taking into account non-typical agricultural elements.

2.2.2. Segmentation

Segments or image objects provide the basis of geospatial object-based image analysis (GEOBIA) (Blaschke, 2010). Out of various object-based image analysis software on the market, we selected the product eCogniton® of Trimble (eCognition Developer, Server version 8.64.1), since it provided a batch processing environment. We prepared 549 tiles with a dimension of 4000×4000 pixels and eight spectral bands, four of COV1 and four of COV2 for segmentation. The basic task of segmentation algorithms is the merging of (image) elements based on homogeneity parameters or on the differentiation to neighbouring regions (heterogeneity) (Schiewe, 2002). eCognition's segmentation relies on a bottom-up region merging technique, which aims at minimizing the weighted heterogeneity ($n \times h$) of resulting image objects, where n is the size of a segment and h a parameter of heterogeneity (Baatz and Schaepe, 2000; Benz et al., 2004). In each step, the pair of adjacent image objects (initially a pixel pair) is merged, which results in the smallest growth of the defined heterogeneity. Heterogeneity is defined as heterogeneity of *colour* (spectral data/grey tone) and *shape*, where *shape* heterogeneity can be divided into heterogeneity of *smoothness* and *compactness* of an object. The merging process stops if the growth exceeds the threshold defined by the scale parameter Ψ. The scale parameter is used to determine the approximate size of objects, although in reality the scale parameter Ψ determines the maximal threshold of heterogeneity allowed to grow objects. For segmentation, the user has the option to determine weights for the colour and shape heterogeneity (and for smoothness and compactness).

For the underlying purpose, the *colour* parameter was considered of highest interest, since patch borders are supposed to be placed in locations where the spectral colour of a remotely sensed image changes and creates heterogeneity. The *shape* parameter was

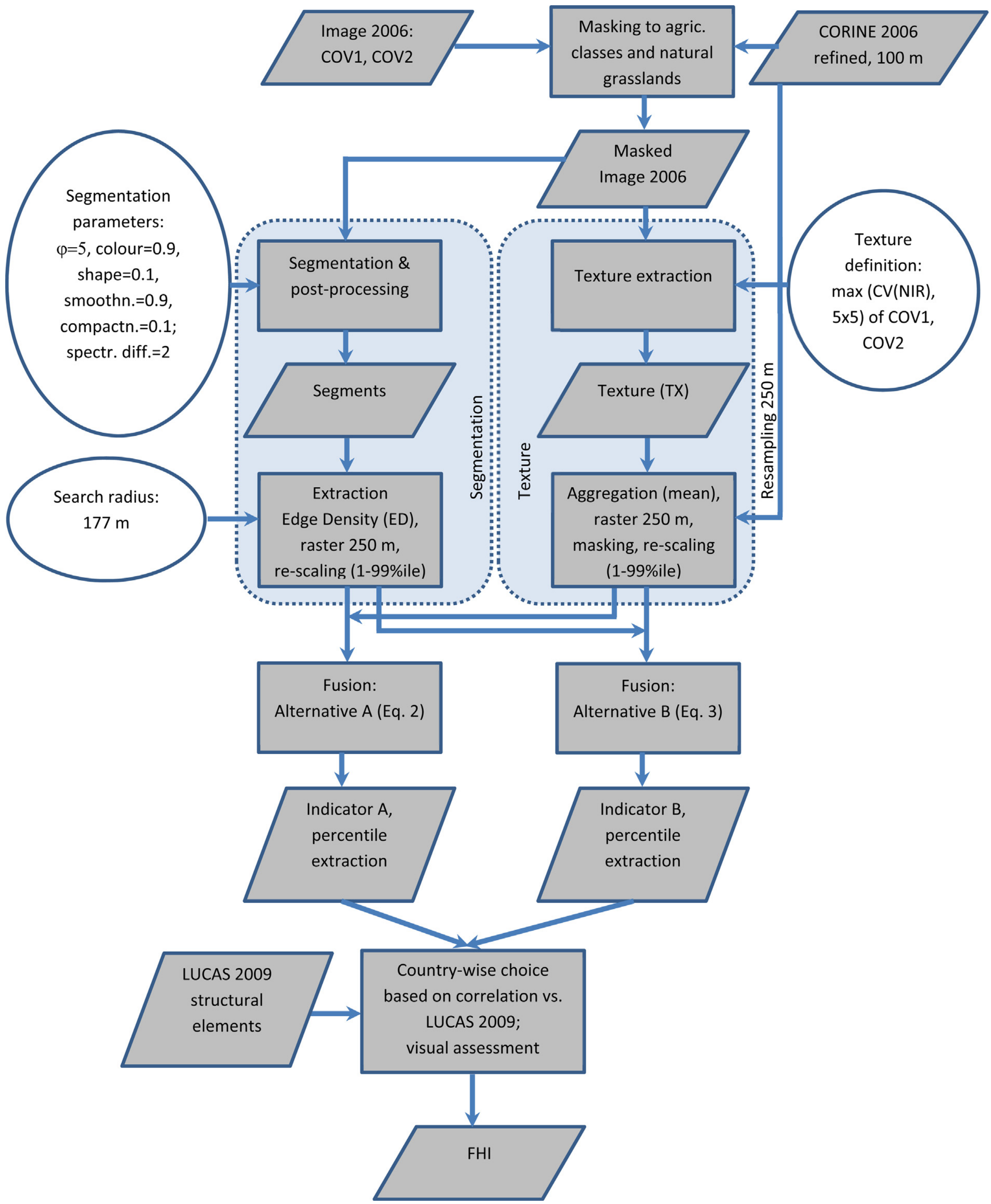

Fig. 1. Overview of the FHI generation, showing input/output data (parallelograms), processes (rectangles), and adopted settings (circles).

considered of minor interest as patches of varying shapes exist, such as very elongated ones, compact and even fragmented ones. We determined the *scale* parameter empirically, testing approximately 20 sites across Europe with different agricultural characteristics, eventually choosing a value on the lower end. We fused segments of very high similarity to larger single elements in a later step, based on spectral difference. This way, the segmentation process delivered a wide range of segment sizes. Generally, we preferred to over-segment the area rather than to under-segment it, since the first would lead to a relative and systematic error, while the latter would lead to fatal results in areas where segments are not captured at all. Also, a following fusion step of spectrally similar objects would increase the size of objects. Since the main aim was the development of a qualitative indicator a minor relative error was accepted.

Before running the segmentation, we masked the dataset for areas other than agricultural land use or natural grassland according to a refined CORINE land cover 2006 product, version 2 (Batista e Silva et al., 2012) with a general minimum mapping unit of 25 ha (locally higher).

We segmented with the following settings: we ran the multi-resolution segmentation process with scale factor = 5, a weight of 0.9 for *colour* and 0.1 for *shape*; we weighted the sub-divisions for *shape* 0.9 for *smoothness* and 0.1 for *compactness.* We applied this rule to all layers with the same weight. We processed the resulting segmentation layer (L1) by the tool "spectral difference", which enabled the fusion of similar objects based on a threshold criterion. We determined the maximum difference to keep separate objects empirically for different regions and set it to 2. Then, we exported to a vector layer and further processed the resulting segmentation layer (L2).

2.2.3. Edge density calculation

We calculated a segmentation edge density for the vector tiles within ESRI ArcGIS (ESRI, 2011) using Python scripts (http://www.python.org). After converting the polygons to lines (edges) we calculated the edge density (ED) per km^2 for 250 m grids. We calculated ED as ED = E/A, where E represents total edge length [km] and A total agricultural area [km^2]. We selected a search radius *r* that circumvented an entire 250 m pixel (i.e. radius $r = 250/2 * \sqrt{(2)} = 177$ m).

2.2.4. Texture calculation

Some regions with very small patches were sometimes not captured by the segmentation process. This occurred especially in areas where patches were not contrasted well from others. The reasons for this failure were visually identified by comparing Google™ Earth imagery to the original images and the preliminary results, and can be reassumed as (i) very small fields which created a high number of (blurred) mixed pixels, (ii) similar crops on small patches without clear border lines or structures or, (iii) low image quality. For those regions the applied approach was apparently at its limits. Although some non-detected patches were smaller (or narrower) than 25 m, yet some of them were clearly larger (or broader) than this size, leaving options for further improvements. Since the potentialities of spectral-based segmentation had been already exploited, we envisaged a complementary texture-based approach. Image texture is commonly defined as the characteristic physical structure given to an object by the size, shape, arrangement, and proportions of its parts (Soille, 2002). Texture is a promising parameter which has been investigated for field size mapping in the past (Kuemmerle et al., 2009). In this work, we extracted texture as relative variance of the near-infrared (NIR) bands, i.e. as coefficient of variation (CV), which is defined as $\sqrt{(\text{variance})}/\text{mean}$. We calculated CV on a 5×5 pixel moving window applied to the near-infrared layers of COV1 and COV2 and finally maximized it to a single value. We considered the calculation of this indicator based on the only NIR bands as a trade-off between data content (vegetation is highly reflected or transmitted in the NIR range) (Jackson and Huete, 1991) and computing time, which helped to keep the calculation time within reasonable time limits. Eventually, we aggregated (applying an arithmetic mean) to 250 m grid cells. To avoid data inconsistencies due to data of non-agricultural land we masked pixels with less than 50% agricultural coverage (or natural grasslands), employing a resampled CORINE land cover mask of 250 m grid size.

2.2.5. Fusion edge density – texture

In the final step we combined both data layers of segmentation and texture to a final indicator (fusion). We first rescaled the values of both layers based on the global 1- and 99-percentile to values between 0 and 1.

$$x_{\text{rescaled},i} = \frac{x_i - 1\,‰}{99\,‰ - 1\,‰} \tag{1}$$

We replaced values less than the 1-percentile or greater than the 99-percentile by 0 and 1 respectively to exclude a distorting effect (outlier-effect) of extreme values.

We designed the fusion in a way to accommodate the trust we had into the layers. Following Bordogna et al., 2012, input data imperfections may be taken into account by the expert if partial data reliability is being defined by partial trust into that layer. A data layer with partial trust is reflected to a minor degree in the fusion product, proportional to the partial trust. Generally we retained both edge density and texture as trusted indicators and we intended to use both data layers for the final indicator. However, empirical tests revealed that texture was for some cases better suited to express the presence of small patches, which was the case when the edge density failed as indicator (in these cases the edge density was low). To improve the results in those cases, we applied the following rule: generally, we expected the rescaled edge density (ED_{resc}) to deliver the same response as the rescaled texture (TX_{resc}). However, if ED_{resc} stayed in magnitude behind TX_{resc} we assumed that ED_{resc} did not capture small patches. As already mentioned above, in this particular case we had less trust in ED_{resc} than in TX_{resc}. In fact, the formula was designed in a way that the loss of trust in ED_{resc} increases with rising difference $TX_{resc} - ED_{resc}$. In logical-mathematical terms, this fusion process can be expressed as:

$$\begin{aligned}
&\text{If } TX_{resc} < ED_{resc} \\
&\text{then FHI} = TX_{resc} * ED_{resc} \\
&\text{else FHI} = TX_{resc}/(1 - (TX_{resc} - ED_{resc})) * ED_{resc}
\end{aligned} \tag{2}$$

This fusion process is hereafter referred to as Alternative A. The term in brackets in the *else*-statement re-dimensions the value of TX_{resc} to a higher value and hence gives it higher importance (higher trust). Since we generally assume ED_{resc} and TX_{resc} to be equally trusted, the divergence (difference) between the two values is taken as trust increasing factor.

After fusion, we re-classified values into quintiles (classes 0+, 20+, 40+, 60+, 80+), also referred to as (20-percentile) classes 1–5, thus class "0+" or class 1 expressing the lowest probability of finding small patches on ground and class "80+" or class 5 expressing the highest probability to encounter small patches on ground. In other words, the FHI expresses a degree of probability to encounter small patches on ground.

Visual expert assessment of the results based on remote sensing images revealed that in particular for areas in Bulgaria/Romania very small fields were often not properly captured. Checking back with the single sub-indicators ED and texture it could be identified that texture did still not get enough weight to properly reflect the situation on ground. The following Alternative B is considered to account better for the texture-related component since it puts more weight on this factor.

Alternative B:

The fusion process of Alternative B should consider the cases where TX is larger than ED. There, TX is amplified with increasing difference (TX − ED), adding this term to TX, and eventually (in comparable re-scaled terms) putting more emphasis on TX than in Alternative A. In logical-mathematical terms, the formula can be written as

$$\begin{aligned}
&\text{If } TX_{resc} < ED_{resc} \\
&\text{then FHI} = TX_{resc} * ED_{resc} \\
&\text{else FHI} = TX_{resc} + (TX_{resc} - ED_{resc})
\end{aligned} \tag{3}$$

After this step we re-classified the results according to quintiles 0+, 20+, 40+, 60+, 80+, in which each class is associated with a rising

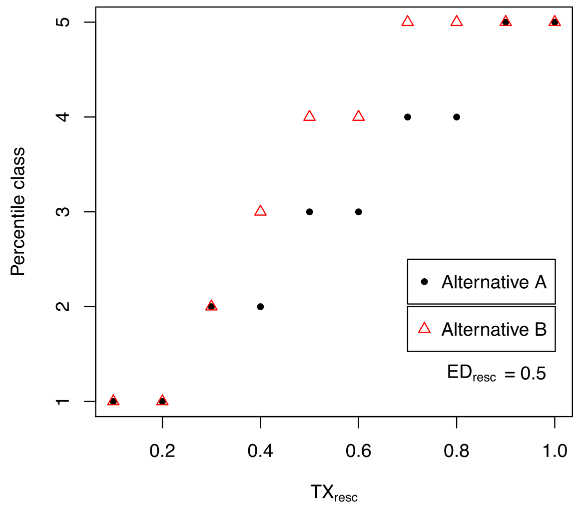

Fig. 2. Comparison of data fusion outcome for Alternative A and B. An example population of 10 TX_{resc} values in the range [0.1,1] and a constant value ED_{resc} of 0.5 was employed.

degree of patch size while containing the same number of samples. A rescaling to values between 0 and 1 could thus be skipped.

As shown in Fig. 2 for an example population, Alternative B provides for a constant ED_{resc} (= 0.5) higher percentile classes compared to Alternative A. This is particularly pronounced at higher ranges of TX_{resc}.

2.2.6. LUCAS driven choice of fusion

LUCAS 2009 is a European-wide area frame survey to gather harmonised data on land use/cover and their changes over time. The 3-year difference to the Image 2006 data was accepted since structural changes on farmland do usually occur slowly, as long as no major event (e.g. political transition, incentive campaign) triggers significant changes. Amongst other data, LUCAS records the occurrence of structural elements, which have been summed up, as listed in Table 1 within a 250 m transect originating at each LUCAS observation point. To find the right choice between Alternatives A and B, we compared the LUCAS data to them. As selection criterion we chose the country-wise correlation coefficient between the number of LUCAS structural elements and the FHI class (average of the four neighbouring pixels). For 21 out of 23 EU countries (EU27 without Bulgaria and Romania, where LUCAS 2009 was not available, and excluding Malta and Cyprus), Alternative A was clearly the better choice. For Italy and Luxembourg, Alternative A and B provided almost equal results. For Bulgaria and Romania we chose the fusion result of Alternative B a priori, since there the peculiarity of the co-occurrence of very big and very small patches was better caught by Alternative B.

Thus, we applied a combined approach, merging the results of Alternative B (for Bulgaria and Romania) with those of Alternative A for all other countries (Alternative AB). It should be kept in mind that the combination of Alternative A and B occurred on the level of classified percentiles, which were calculated for all of Europe.

2.2.7. Association of approximate patch size

The qualitative indicator provided a good means to distinguish agricultural land; however, we developed the indicator further to a semi-quantitative one, associating with each of the qualitative classes the mean (plus lower and upper limit) object size identified during the segmentation process. The derivation of the object size was performed exclusively on pixels, whose quintile-based classes were not altered after the fusion process of edge density and texture. This way, only pure segmentation-based data and no textural data is assessed to derive plot size. However, finally we attributed patch size to all pixels, assuming that the quintile-based classification based on segmentation and texture delivers a comparable valuable class ranking as the sole segmentation-based approach.

Next to an average patch size value for each class, we derived the (lower and upper) class limits. If class limits were taken as minimum and maximum values of patch size of each class, they would overlap, which is not desirable. Therefore, class limits were re-defined in a way that the lower percentile x of a class y is closest to the higher percentile $1-x$ of a class y+1. For instance, class limits between class 0+ (largest patches) and class 20+ (second largest patches) are supposed to be where the percentile x of class 0+ is closest to (the complementary) percentile $1-x$ of class 20+.

2.3. Verification – methods

Verification of the results occurred on different scales for both qualitative and semi-quantitative results.

(1) *ESDAC*: The European Soil Data Centre (ESDAC) has derived field size based on the Image 2000 dataset (http://eusoils.jrc.ec.europa.eu/library/themes/erosion/winderosion/Resources/AvFieldSize.pdf). The ESDAC approach only considers large fields (neglecting small ones), since this data has been designed as input for wind erosion modelling on a European scale. The difference between the two data sets mainly consists in the inclusion of textural analysis in the FHI in order to account for small fields. We carried out a numerical country-wise comparison.
(2) *LUCAS*: The database LUCAS 2009 provides point data on field size for 25 EU member states. The survey assigns the classes 1–4 to each sample of a point grid of 2 km distance, equivalent to the local field plot size of L_a < 0.5 ha, 0.5 ha ≤ L_a < 1 ha, 1 ≤ L_a < 10 ha, and L_a ≥ 10 ha. We compared these classes to FHI-derived field classes.
(3) *IACS*: we carried out a similar comparison on a regional scale, which is illustrated in Fig. 7B. Rintelen and Zenger (2001) reported for Bavaria, a Southern German region with a size of 70,550 km^2 with an agricultural share of 50% the distribution of arable field sizes for the year 1999. Source of their reporting was the InVeKoS data base, an IACS database (Integrated Administration and Control System, EC, 2009) to administer agricultural subsidies.

3. Results

3.1. Farmland Heterogeneity Indicator (FHI)

Fig. 3 illustrates input data, Image 2006, which shows a distinct pattern of small and large patches. In this example, agricultural land surrounding urbanized areas (masked areas in Fig. 3B–D) shows a higher density of small patches. The segmentation and the ED derived thereof did not fully capture this particularity (A and C), while texture is able to distinguish these areas more distinctly (compare B and C, where C is predominantly covered by percentile class 0+). This is reflected in the FHI (D). Fig. 4 shows the FHI for Europe. The historical border between the states of the former Eastern Bloc and the Western countries is clearly visible (e.g. between East and West Germany). Large parts of the Iberian Peninsula are dominated by large patches, which can be explained by historical reasons (*minifundio* in the North versus *latifundio* in the South, Gjelten, 1984). The detail, depicting a

Table 1
Structural elements extractable from LUCAS database 2009.

LUCAS code	Description
1	Grass margins less than 3 m
2	Heath-Shrub tall herb fringes less than 3 m
10	Single bushes single tree
11	Avenue trees
12	Conifer hedges less than 3 m
13	Bush-tree hedges-coppices visibly managed (e.g. pollarded) less than 3 m
14	Bush-tree hedges – not managed – with single Trees – or shrub land deriving from abandonment less than 3 m
15	Grove-Woodland margins (if no hedgerow) less than 3 m
21	Dry stone walls
23	Fences
31	Ditches – channels less than 3 m
32	Rivers – streams less than 3 m
41	Ponds – wetlands less than 3 m
51	Rock outcrops with some natural vegetation
61	Tracks
62	Roads
63	Railways
71	Other linear elements

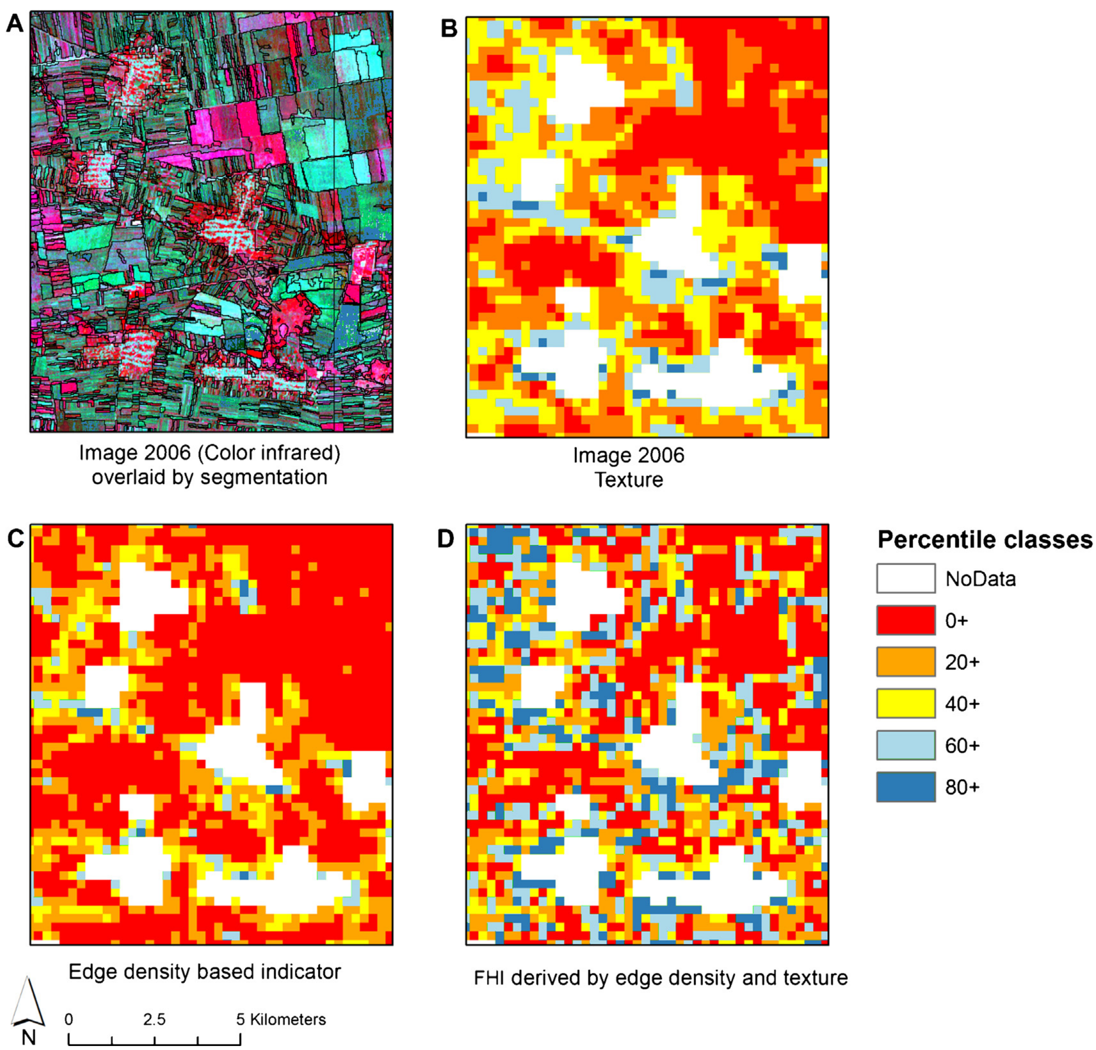

Fig. 3. Intermediate and final products for an area in Romania (Alternative AB) during the generation of the FHI: Input data Image 2006 overlaid by segments (A), texture indicator (B), urban areas are masked, a patch indicator derived by edge density only (C), definitive FHI using edge density and texture (D).

subset of the Italian Po Valley, shows a hot spot of large patches on the left side, which is in fact an area of large rice paddies. Averaged over EU27, FHI values were calculated for all agricultural CLC classes including 'natural grasslands' (Fig. 5). Based on CLC classification, agroforestry areas clearly result as areas with largest patch size (low FHI), followed by Olive groves and natural grasslands. On the other hand, pastures and mixed (heterogeneous) CLC classes are detected as areas with smallest patch size (high FHI). Intermediate values were found for typical arable land and all other permanent vegetation.

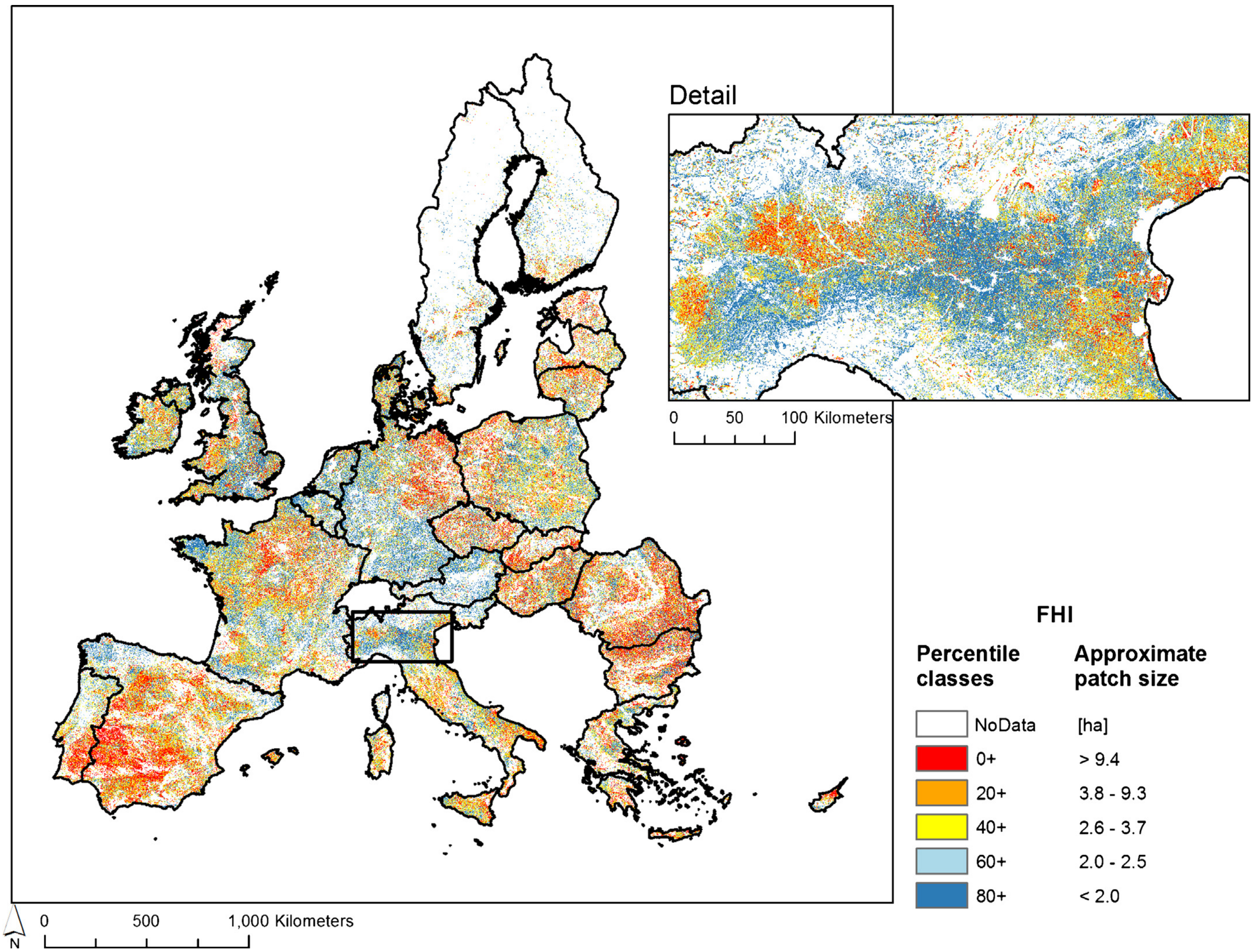

Fig. 4. FHI for Europe (EU27), Alternative AB. The detail shows the FHI for the agricultural area around the Po River in Northern Italy.

3.2. Approximate patch size

The approximate patch size limits (lower and upper limits) of each class are reported in Table 2. The term *approximate* patch size is preferred due to data's inherent uncertainty. The class percentiles of where class limits have been detected and a reliability of each class limit is given. Class limits are assumed to occur where the histograms of neighbouring classes intersect. The reliability measure expresses the population fraction of two neighbouring classes that can be expected to fall into the two classes with the specified limits, i.e. the percentiles of two neighbouring classes, expressing the positively associated population with each class, are averaged.

3.3. Verification – results

3.3.1. ESDAC

The results of the numerical country-wise comparison with ESDAC field size data are displayed for some countries in Fig. 6. Only the results of France (FR), Spain (ES) and Germany (DE) are displayed in Fig. 6 since they dispose of reasonable ranges (FHI range > 2.5, ESDAC field size range > 18 ha) and sufficient points per country ($n > 40$). Low field size coincides with high FHI classes and vice versa. The most reliable comparison is the one for Germany, which covers a broader range for both FHI and field size and consists of a higher number of points. For Germany, the correlation coefficient has been calculated as $R = -0.74$.

3.3.2. LUCAS

The coincidence between the class limits of FHI and LUCAS (L_a) is not perfectly congruent, as Table 3 shows. FHI class 1 and LUCAS class 4 fit best where there are slight deviations between their classes' field plot sizes for the other pairs. However, an accumulative comparison for the study site shows good agreement between the FHI and LUCAS (Fig. 7A).

3.3.3. IACS

For Bavaria high congruency of different field plot sizes was found (Fig. 7B). Agreements were better for medium-sized patches (>2 ha) than for those less than 2 ha. For congruent comparison between FHI and the reported data, interpolation of reported data was performed applying a polynomial degree 3 ($R^2 = 0.99$).

Although an overall numerical assessment of all three verifications can hardly be calculated, in all cases the plausibility of the results is documented. This is particularly advantageous as comparisons have been made across regional, national and continental scales.

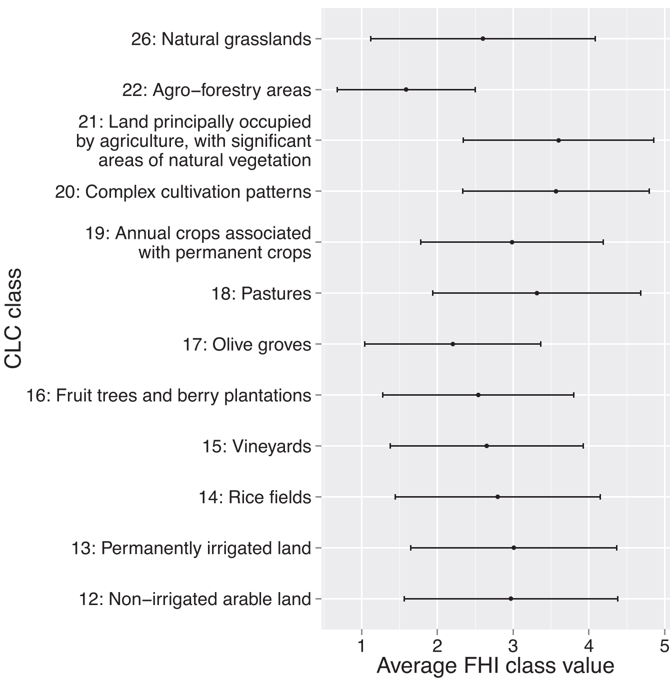

Fig. 5. Average FHI values (and standard deviation) of agricultural CLC classes (level 3) and 'natural grasslands' (EU27) for Alternative AB.

4. Discussion

To our knowledge, this paper presents the first-fully observed Farmland Heterogeneity Indicator at a continental level. The indicator assesses the density of field edges or other structural elements that delineate agricultural patches (roads, buildings, etc.) and are detectable from satellite-based spectral remote sensing data for agricultural lands. The FHI fills the gap of a so far missing detailed, harmonized continental indicator on a landscape scale for farmland heterogeneity, allowing or contributing, amongst others, to an ecological assessment of agricultural land in terms of ecosystem service potential and farmland biodiversity . With reference to other works on the identification of linear features (García-Feced et al., 2015; Van der Zanden et al., 2013), the main differences consist in the wider definition of mapping features, the identification of the patch as reference landscape unit and the focus on landscape configurational heterogeneity.

Methodologically, edges or structural elements are detected due to existing visible structures or spectral differences between fields, or they can be inferred by the presence of elevated texture values. The latter applies in particular to areas of very small patches, where field edges cannot be individually detected due to sensor resolution. For the derivation of FHI, the appraised approach of Chica-Olmo and Abarca-Hernández (2000), namely the combination of segmentation and texture-based data, was followed. The integration of these data represents an added value compared to other indices computed for the European continent, e.g. as for the mentioned ESDAC-based field size. The parallel approach offers advantages, such as more consolidated and robust results, or an

Table 3
Corresponding FHI and LUCAS classes.

FHI		LUCAS	
Class	Area [ha]	Class	Area L_a [ha]
1	>9.4	4	>10
2 + 3 + 4	2.0–9.3	3	1–10
5	<2.0	2	0.5–1

Table 2
Percentile class specific characteristics. Percentile and patch size limits of classes and a reliability measure is shown.

<table>
<tr><th></th><th>Class 0+</th><th colspan="2">Class 20+</th><th colspan="2">Class 40+</th><th colspan="2">Class 60+</th><th>Class 80+</th></tr>
<tr><th></th><th colspan="8">Limit</th></tr>
<tr><th></th><th>Lower</th><th>Upper</th><th>Lower</th><th>Upper</th><th>Lower</th><th>Upper</th><th>Lower</th><th>Upper</th></tr>
<tr><td>Percentile</td><td>0.24</td><td>0.76</td><td>0.37</td><td>0.63</td><td>0.40</td><td>0.60</td><td>0.39</td><td>0.61</td></tr>
<tr><td>[ha]</td><td>9.2</td><td>9.6</td><td>3.8</td><td>3.8</td><td>2.6</td><td>2.7</td><td>2.0</td><td>2.0</td></tr>
<tr><td>Avg. class limit [ha]</td><td colspan="2">9.4</td><td colspan="2">3.8</td><td colspan="2">2.7</td><td colspan="2">2.0</td></tr>
<tr><td>Reliability</td><td colspan="2">0.76</td><td colspan="2">0.63</td><td colspan="2">0.60</td><td colspan="2">0.61</td></tr>
</table>

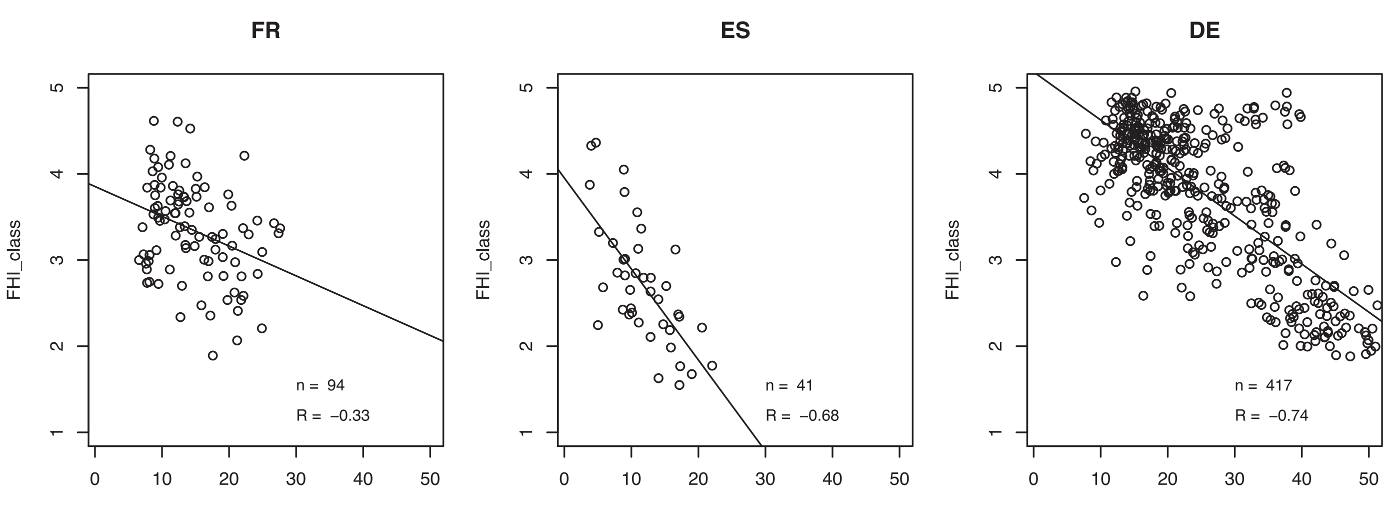

Fig. 6. Scatterplot FHI (Alternative AB) versus field size according to ESDAC for three EU-countries.

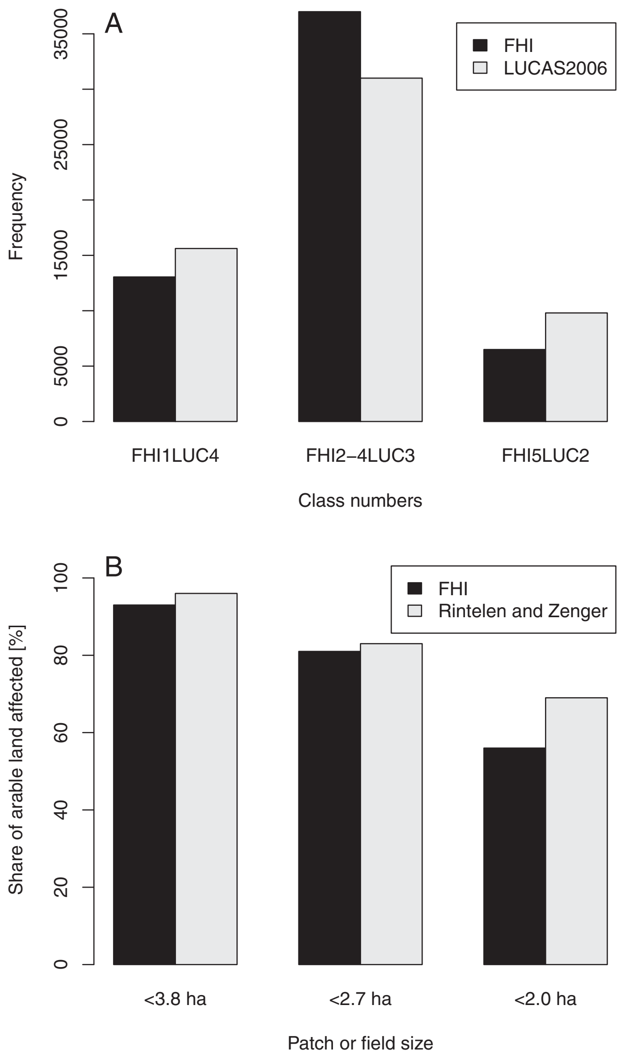

Fig. 7. (A) Comparison of FHI classes with LUCAS field size classes. Numbers of FHI and LUCAS classes are depicted below each bar pair. (B) Comparison of FHI based and IACS based cumulative shares of arable land covered by different field sizes for Bavaria (Germany).
Source: InVeKos (Rintelen and Zenger, 2001).

asymmetric and dynamic assessment of "trust" of the single layers, but requires a more complex process of data fusion.

A valuable advantage of FHI is that the whole area is assessed by a harmonized approach, although for Bulgaria/Romania a slightly modified approach had to be applied due to local peculiarities. To achieve this, a landscape metric's-based approach was employed, allowing the indicator computation of a large geographic region within reasonable time. The indicator is of qualitative nature, yet an effort was made to associate semi-quantitative information by delivering 5 classes of varying patch size degrees within agricultural land (including grasslands). The outcome is characterized by the trade-off between spatial resolution and coverage: the data set's spatial resolution can be insufficient in the case of very small/narrow patches (limitation), but it is to date a unique data source providing European coverage, essential for a harmonized European assessment. The availability of two temporal coverages (COV1 and COV2) is advantageous, as it is increasing the probability to encounter vegetated fields on ground for at least one date, which is expected to enhance patch detection compared to uncultivated patches or bare soil.

The approach is repeatable if, given the single processing steps documented here, similar data are available. This includes at least a remote sensing data set with comparable characteristics and an updated land use/land cover mask. It is highly probable that these data will be available for the coming years, provided by the CORINE project and by recent or upcoming sensors (e.g. Sentinel-2, Landsat-8, etc.). Exactly identical data input settings will hardly be encountered in future. This, however, should not impede a re-run, considering that it is not the single pixel but pattern changes which are usually of interest to decision makers. Monitoring or change detection will be possible through the extraction of data population values (e.g. FHI before classification, or patch size) at defined limits (e.g. percentiles) at time 1, and superimposition of these values to corresponding data population values at time 2, getting the percentile rank (Schultzkie, 2013). Class volume differences will then deliver the direction, degree and the geo-locations of changes. The percentile-based approach and the rescaling (Eq. (1)) do technically not facilitate repeatability but enhance certainly the robustness of the indicator, also in view of future comparability.

The results have been verified on different scales (regional, national and continental) and for different areas in Europe. Good agreement with reported field sizes of three independent sources was found for FHI, confirming the plausibility of the results. Despite the good agreement for FHI, the uncertainty of the underlying derived patch size remains high, for which in particular the derived approximate field size has to be considered of indicative order. In general, main sources of uncertainty are linked to (i) the inherent characteristics and limitations of the multispectral remote sensing data used, (ii) the segmentation settings, (iii) the generalization process of CORINE land use/land cover map. Field size estimation uncertainties relate to the necessity to extract patch size from the areas which are purely derived by segmentation, and the technique and assumption made to extract field class limits. Moreover, the assessment is based on all detected elements within agricultural land, including minor areas of semi-natural or natural origin, and impervious areas.

Overall, the FHI can provide a useful data source for agro-economic assessments, for example, as input for an ecological and economic assessment of energy/machinery use or status of land consolidation. It is noteworthy that a context-based view is required for a correct interpretation of results. Large patches within typical agroforestry areas (as e.g. found in Southern Iberia) do not have the same ecological potential of large patches within an intensive agricultural area (e.g. East Germany). Additional data is required to further analyze the indicator. For example, to distinguish the above-mentioned cases, land use/land cover data or an indicator describing patch complexity would help (i.e. arable parcels generally have a more simple and geometric shape than agroforestry patches); the latter could be derived from the same base data.

Considering the importance of small fields, structured landscapes and the presence of field margins, following Fahrig et al. (2015) and their work on configurational heterogeneity of farmland, FHI may serve as an input for farmland biodiversity assessments.

For the future, a quantitative indicator of patch size should be envisaged for Europe. In the ideal case, such an indicator would be based on improved data input, such as optical remote sensing data in the range of 2–10 m.

5. Conclusions

The FHI is a novel indicator to characterize the agricultural landscape, providing information on configurational heterogeneity. Being based both on the occurrence of spectral differences between adjacent elements and on textural information, it (i) expresses the presence of visible field borders and other structural elements within a field in qualitative terms, and (ii) provides the basis for an indicative field size. To our knowledge, and taking into account previous work carried out by Van der Zanden et al. (2013), the work presented in this paper is the first pan-European mapping of *observed* farmland structural heterogeneity at a detailed scale. Compared to existing applications, the combination of spectral and texture information enhances robustness of the resulting indicator, which is characterized by a higher accuracy than the single components on their own. However, it has to be kept in mind that due to scale dependency, very small or narrow elements are not captured by the used sensor (e.g. single trees). Moreover, the applied methodology identifies transition zones of changing land use/land cover, which do not necessarily represent or correspond with cadastral limits. Potential fields of application concern the Common Agricultural Policy and its greening package, farmland biodiversity assessments as well as ecosystem service mapping. The FHI is a snapshot of the situation at a specific date, but repeatable in time while allowing monitoring landscape structural changes.

Acknowledgements

Special thanks to Pierre Soille and Roeland de Kok for their help and fruitful discussions about this issue. Many thanks also to René Beuchle and Michael Vollmar, who assisted works for the image segmentation.

References

Baatz, M., Schaepe, A., 2000. Multiresolution Segmentation: an optimization approach for high quality multi-scale image segmentation. In: Strobl, J., Blaschke, T., Griesebner, G. (Eds.), Angewandte Geographische Informations-Verarbeitung XII. Beitraege zum AGIT-Symposium Salzburg 2000. , pp. 12–23 (German Edition).
Batista e Silva, F., Lavalle, C., Koomen, E., 2012. A procedure to obtain a refined European land use/cover map. J. Land Use Sci., 1–29, http://dx.doi.org/10.1080/1747423X.2012.667450.
Benton, T.G., Vickery, J.A., Wilson, J.D., 2003. Farmland biodiversity: is habitat heterogeneity the key? Trends Ecol. Evol. 18, 182–188, http://dx.doi.org/10.1016/S0169-5347(03)00011-9.
Benz, U.C., Hofmann, P., Willhauck, G., Lingenfelder, I., Heynen, M., 2004. Multi-resolution, object-oriented fuzzy analysis of remote sensing data for GIS-ready information. ISPRS J. Photogram. Rem. Sens. 58, 239–258, http://dx.doi.org/10.1016/j.isprsjprs.2003.10.002.
Billeter, R., Liira, J., Bailey, D., Bugter, R., Arens, P., Augenstein, I., Aviron, S., Baudry, J., Bukacek, R., Burel, F., Cerny, M., De Blust, G., De Cock, R., Diekötter, T., Dietz, H., Dirksen, J., Dormann, C., Durka, W., Frenzel, M., Hamersky, R., Hendrickx, F., Herzog, F., Klotz, S., Koolstra, B., Lausch, A., Le Coeur, D., Maelfait, J.P., Opdam, P., Roubalova, M., Schermann, A., Schermann, N., Schmidt, T., Schweiger, O., Smulders, M.J.M., Speelmans, M., Simova, P., Verboom, J., Van Wingerden, W.K.R.E., Zobel, M., Edwards, P.J., 2008. Indicators for biodiversity in agricultural landscapes: a pan-European study. J. Appl. Ecol. 45, 141–150, http://dx.doi.org/10.1111/j.1365-2664.2007.01393.x.
Blaschke, T., 2010. Object based image analysis for remote sensing. ISPRS J. Photogram. Rem. Sens. 65, 2–16, http://dx.doi.org/10.1016/j.isprsjprs.2009.06.004.
Bommarco, R., Kleijn, D., Potts, S.G., 2013. Ecological intensification: harnessing ecosystem services for food security. Trends Ecol. Evol. 28, 230–238, http://dx.doi.org/10.1016/j.tree.2012.10.012.
Bordogna, G., Boschetti, M., Brivio, P.A., Carrara, P., Stroppiana, D., Weissteiner, C.J., 2012. Handling heterogeneous bipolar information for modelling environmental syndromes of global change. Environ. Model. Softw. 36, 131–147, http://dx.doi.org/10.1016/j.envsoft.2012.03.016.
Chica-Olmo, M., Abarca-Hernández, F., 2000. Computing geostatistical image texture for remotely sensed data classification. Comput. Geosci. 26, 373–383, http://dx.doi.org/10.1016/S0098-3004(99)00118-1.
Donald, P.F., Sanderson, F.J., Burfield, I.J., van Bommel, F.P.J., 2006. Further evidence of continent-wide impacts of agricultural intensification on European farmland birds, 1990–2000. Agric. Ecosyst. Environ. 116, 189–196, http://dx.doi.org/10.1016/j.agee.2006.02.007.
EC, 2009. Council Regulation (EC) No 73/2009. Common rules for direct support schemes for farmers under the common agricultural policy and establishing certain support schemes for farmers.
EEA, 2007. CLC2006 technical guidelines (EEA Technical report No. 17/2007). Office for Official Publications of the European Communities, European Environmental Agency (EEA), Luxembourg.
Ernoult, A., Bureau, F., Poudevigne, I., 2003. Patterns of organisation in changing landscapes: implications for the management of biodiversity. Landsc. Ecol. 18, 239–251, http://dx.doi.org/10.1023/A:1024457031235.
ESRI, 2011. ArcGIS Desktop: Release 10. Environmental Systems Research Institute, Redlands, CA.
European Commission, 2011. Our life insurance, our natural capital: an EU biodiversity strategy to 2020. COM (2011) 244, Brussels.
European Union, 2013. Regulation (EU) No 1307/2013 of the European Parliament and of the Council of 17 December 2013 establishing rules for direct payments to farmers under support schemes within the framework of the common agricultural policy and repealing Council Regulation (EC) No 637/2008 and Council Regulation (EC) No 73/2009. Official Journal of the European Union L 347/608.
Fahrig, L., Girard, J., Duro, D., Pasher, J., Smith, A., Javorek, S., King, D., Lindsay, K.F., Mitchell, S., Tischendorf, L., 2015. Farmlands with smaller crop fields have higher within-field biodiversity. Agric. Ecosyst. Environ. 200, 219–234, http://dx.doi.org/10.1016/j.agee.2014.11.018.
Forman, R.T.T., 1995. Land Mosaics: The Ecology of Landscapes and Regions. Cambridge Press, Cambridge, UK.
Gabriel, D., Roschewitz, I., Tscharntke, T., Thies, C., 2006. Beta diversity at different spatial scales: plant communities in organic and conventional agriculture. Ecol. Appl. 16, 2011–2021, http://dx.doi.org/10.1890/1051-0761(2006)016[2011:BDADSS]2.0.CO;2.
García-Feced, C., Weissteiner, C.J., Baraldi, A., Paracchini, M.L., Maes, J., Zulian, G., Kempen, M., Elbersen, B., Pérez-Soba, M., 2015. Semi-natural vegetation in agricultural land: European map and links to ecosystem service supply. Agron. Sustain. Dev. 35, 273–283, http://dx.doi.org/10.1007/s13593-014-0238-1.
Gjelten, T., 1984. To Improve Spanish Farming Without Hurting Spanish Farmers. The Arkleton Trust, Arkleton, Langholm, Scotland.
Haenke, S., Kovács-Hostyánszki, A., Fründ, J., Batáry, P., Jauker, B., Tscharntke, T., Holzschuh, A., 2014. Landscape configuration of crops and hedgerows drives local syrphid fly abundance. J. Appl. Ecol. 51, 505–513, http://dx.doi.org/10.1111/1365-2664.12221.
Hamer, T.L., Flather, C.H., Noon, B.R., 2006. Factors associated with grassland bird species richness: the relative roles of grassland area, landscape structure, and prey. Landsc. Ecol. 21, 569–583, http://dx.doi.org/10.1007/s10980-005-2167-5.
Herzog, F., Steiner, B., Bailey, D., Baudry, J., Billeter, R., Bukácek, R., De Blust, G., De Cock, R., Dirksen, J., Dormann, C.F., De Filippi, R., Frossard, E., Liira, J., Schmidt, T., Stöckli, R., Thenail, C., Van Wingerden, W., Bugter, R., 2006. Assessing the intensity of temperate European agriculture at the landscape scale. Eur. J. Agron. 24, 165–181, http://dx.doi.org/10.1016/j.eja.2005.07.006.
Jackson, R.D., Huete, A.R., 1991. Interpreting vegetation indices. Prev. Vet. Med. 11, 185–200, http://dx.doi.org/10.1016/S0167-5877(05)80004-2.
Jentsch, A., Steinbauer, M.J., Alt, M., Retzer, V., Buhk, C., Beierkuhnlein, C., 2012. A systematic approach to relate plant-species diversity to land use diversity across landscapes. Landsc. Urban Plan. 107, 236–244, http://dx.doi.org/10.1016/j.landurbplan.2012.06.012.
Kaule, G., Krebs, S., 1989. Creating new habitats in intensively used farmland. In: Buckley, G.P. (Ed.), Biological Habitat Reconstruction, Belhaven Press, London, pp. 161–170.
Kuemmerle, T., Hostert, P., St.-Louis, V., Radeloff, V.C., 2009. Using image texture to map farmland field size: a case study in Eastern Europe. J. Land Use Sci. 4, 85–107, http://dx.doi.org/10.1080/17474230802648786.
Landis, D.A., Wratten, S.D., Gurr, G.M., 2000. Habitat management to conserve natural enemies of arthropod pests in agriculture. Annu. Rev. Entomol. 45, 175–201, http://dx.doi.org/10.1146/annurev.ento.45.1.175.
Le Féon, V., Schermann-Legionnet, A., Delettre, Y., Aviron, S., Billeter, R., Bugter, R., Hendrickx, F., Burel, F., 2010. Intensification of agriculture, landscape composition and wild bee communities: a large scale study in four European countries. Agric. Ecosyst. Environ. 137, 143–150, http://dx.doi.org/10.1016/j.agee.2010.01.015 (Spec. Sect. Harvest. Perenn. Grassl. Ecol. Models Farmings Perenn. Future).
MA, 2005. Millennium Ecosystem Assessment. Ecosystems and Human Well-being: Synthesis. Island Press, Washington, DC.
Marshall, E.J.P., Moonen, A.C., 2002. Field margins in northern Europe: Their functions and interactions with agriculture. Agric. Ecosyst. Environ. 89, 5–21, http://dx.doi.org/10.1016/S0167-8809(01)00315-2.
Overmars, K.P., Schulp, C.J.E., Alkemade, R., Verburg, P.H., Temme, A.J.A.M., Omtzigt, N., Schaminée, J.H.J., 2014. Developing a methodology for a species-based and spatially explicit indicator for biodiversity on agricultural land in the EU. Ecol. Indic. 37A, 186–198, http://dx.doi.org/10.1016/j.ecolind.2012.11.006.
Paracchini, M.L., Petersen, J.-E., Hoogeveen, Y., Bamps, C., Burfield, I., van Swaay, C., 2008. High Nature Value Farmland in Europe – An Estimate of the Distribution Patterns on the Basis of Land Cover and Biodiversity Data (No. EUR 23480 EN). Office for Official Publications of the European Communities, JRC, IES, Luxembourg.
Rintelen, P.-M., Zenger, X., 2001. Neue Ansaetze zum Tausch landwirtschaftlicher Flaechen. Sch. Berat. SuB 5, 50–53.
Roschewitz, I., Hücker, M., Tscharntke, T., Thies, C., 2005. The influence of landscape context and farming practices on parasitism of cereal aphids. Agric. Ecosyst. Environ. 108, 218–227, http://dx.doi.org/10.1016/j.agee.2005.02.005.
Rydberg, A., Borgefors, G., 2001. Integrated method for boundary delineation of agricultural fields in multispectral satellite images. IEEE Trans. Geosci. Rem. Sens. 39, 2514–2520, http://dx.doi.org/10.1109/36.964989.
Schiewe, J., 2002. Segmentation of high-resolution remotely sensed data – concepts, applications and problems. In: Presented at the Symposium on Geospatial Theory, Processing and Applications, Ottawa.
Schultzkie, L., 2013. Percentiles and More Quartiles. Oswego City School District Regents Exam Prep Center, http://regentsprep.org/REgents/math/ALGEBRA/AD6/quartiles.htm (accessed 15.09.15).

Soille, P., 2002. Morphological texture analysis: an introduction. In: Mecke, K., Stoyan, D. (Eds.), Morphology of Condensed Matter, Lecture Notes in Physics. Springer, Berlin, Heidelberg, pp. 215–237.

Soille, P. (Ed.), 2008. The Image-2006 mosaic project (No. EUR 23755 EN), JRC Scientific and Technical Reports. European Commission, Luxembourg.

Tscharntke, T., Klein, A.M., Kruess, A., Steffan-Dewenter, I., Thies, C., 2005. Landscape perspectives on agricultural intensification and biodiversity – ecosystem service management. Ecol. Lett. 8, 857–874, http://dx.doi.org/10.1111/j.1461-0248.2005.00782.x.

Van der Zanden, E.H., Verburg, P.H., Mücher, C.A., 2013. Modelling the spatial distribution of linear landscape elements in Europe. Ecol. Indic. 27, 125–136, http://dx.doi.org/10.1016/j.ecolind.2012.12.002.

Wagner, H.H., Wildi, O., Ewald, K.C., 2000. Additive partitioning of plant species diversity in an agricultural mosaic landscape. Landsc. Ecol. 15, 219–227, http://dx.doi.org/10.1023/A:1008114117913.

Wiens, A.J., Stenseth, N.C., Van Horne, B., Ims, R.A., 1993. Ecological mechanisms and landscape ecology. Oikos 66, 369–380, http://dx.doi.org/10.2307/3544931.